

***In silico* study on the contribution of the follicular route to dermal permeability of small molecules.**

Daniel Sebastia-Saez¹, Guoping Lian², Tao Chen¹

¹School of Chemistry and Chemical Engineering, University of Surrey, Guildford, United Kingdom

²Unilever R&D Colworth, Bedford, United Kingdom

*Corresponding author: Tao Chen (t.chen@surrey.ac.uk)

Abstract

Purpose. This study investigates *in silico* the effect that physico-chemical parameters have on the contribution of the hair follicle to overall dermal permeability of small molecules, as published experimental work provides inconclusive information on this matter.

Methods. We use a validated transdermal permeation mechanistic model. A parametric study is conducted varying physico-chemical parameters such as lipophilicity, molecular weight, protein binding, compound ionisation and *pH*. The simulated data is compared to published experimental data to discuss how those properties can modulate dermal permeation.

Findings. The results indicate that the contribution of the follicular route to dermal permeation can range from negligible to major depending on the properties of the substance filling the follicular route and the chemical compound being administered. Lipophilicity and molecular weight are confirmed to have a strong effect. In a lipophilic follicular route, the effect of *pH* and ionisation proves significant too.

Conclusions. Careful characterisation of the substance filling the follicular route would be recommended prior to conducting experimental work of dermal permeation for small molecules, as changes between *in vivo* and *in vitro* due to handling of samples and cessation of vital functions can affect significantly how the follicular route contributes to overall dermal permeation, hence hindering data interpretation.

1. Introduction

Understanding the mechanisms behind dermal permeation of chemicals is of high importance to the pharmaceutical and cosmetic industries, as well as for risk assessment of chemical exposure. Reported experimental studies have shown that the follicular route (FR) contributes significantly to dermal permeation (Knorr et al., 2006). This can be explained as the anatomy of the FR offers large surface area for mass transport due to an enfolding around the hair, which extends deeply into the dermis (De), hence by-passing the stratum corneum (SC) as the skin's main barrier. Published experimental data is inconclusive on the mechanisms behind the role of the FR on overall dermal permeability, with implications on the general understanding of the delivery and safety of dermal formulations. Table 1 summarises studies on dermal permeability through the FR published in the last two decades. While these studies agree that the FR plays an important role, further clarification is required regarding the role of the physico-chemical properties of both the FR and the chemicals administered, such as lipophilicity, molecular weight, ionisation, et cetera. For example, Otberg et al. (2008) found that the FR significantly increases the concentration of caffeine (a hydrophilic compound) in plasma in their *in vivo* experiments with caffeine. As opposed to the results observed, the FR should not contribute significantly to the permeability of caffeine, as it would be reasonable to assume that the FR has a lipophilic character *in vivo* by virtue of the continuous secretion of sebum by the sebaceous gland.

Teichmann et al. (2007) observed that a lipophilic compound (curcumin, $\log K_{o/w}=3.30$) permeated into the skin through the FR and the lipidic gaps in the SC in their *in vivo* experiments, but not through the hydrophilic keratinocytes. In this instance, the experiments would be in accordance with currently accepted knowledge on the postulated lipophilic character of the FR *in vivo*.

Similarly, inconclusive results can be observed in the literature when comparing experiments carried out *in vitro* and *ex vivo*, where the sebaceous gland has ceased to produce sebum. Specimens are often soaked in aqueous solutions (e.g., PBS) prior to *ex vivo* and *in vitro* permeation experiments, which together with freezing and thawing of samples can contribute to altering the physico-chemical properties of the substance filling the FR. These alterations would suggest that the permeation of hydrophilic compounds could be favoured *in vitro* or *ex vivo* as opposed to *in vivo*. For example, Genina et al. (2002) studied the permeation of a lipophilic compound (Dye Indigo Carmine, $\log K_{o/w} = 3.72$) and a hydrophilic compound (Dye Indocyanina Green, $\log K_{o/w} = -0.79$), showing that the hydrophilic compound permeates faster than the lipophilic compound *in vitro*. This would be expected according to the postulated physico-chemical changes taking place during *in vitro* sample preparation. Grams and Bouwstra (2002) however, detected the presence of lipophilic compounds in the FR after their *ex vivo* permeation experiments, but not hydrophilic ones, suggesting that the FR favours the permeation of lipophilic compounds even when sebum secretion has ceased. These results could be explained as arguably *ex vivo* experiments mimic *in vivo* conditions more closely than *in vitro* tests (i.e., a significant amount of sebum could still be present in the FR).

Mohd et al. (2016) and Frum et al. (2007) directly compared the contribution of the FR on the overall skin permeation for a set of compounds with a significant range of $\log K_{o/w}$ *in vitro*. However, the contribution of the FR was obtained using different methodologies in both studies. While Frum et al. (2007) used the skin sandwich technique in their experiments, Mohd et al. (2016) opted for wax plugging half of the hair follicles in their skin samples. Mohd et al. (2016) observed that the contribution of the FR to dermal permeability was noticeably greater for hydrophilic compounds. Their results suggest thus that the FR favours the permeation of hydrophilic compounds *in vitro*. Frum et al. (2007) also provided direct comparison between the contribution of the FR against $\log K_{o/w}$ for a set of chemicals *in vitro*. In this instance, the opposite trend was observed at low values of $\log K_{o/w}$, with a turning point at $\log K_{o/w}=1.25$. Their results show that the FR does not play a relevant role for both strongly hydrophilic and strongly lipophilic molecules. For moderately lipophilic and hydrophilic compounds however, the FR appears to be relevant. Frum et al. (2007) conclude that not the lipophilicity, but other molecular properties, play an important role on the contribution of the FR on dermal permeability.

The above suggests that a standard rationale to measure the contribution of the FR to overall dermal permeation is needed, as well as a complete analysis of the effect of the several parameters involved on the role of the FR on overall dermal permeability. Published experimental data consulted suggest that both the molecular weight and the lipophilicity play a substantial role. However, quantification and further investigation on how other parameters are involved in the process is currently needed. It is hypothesized that, not only molecular weight and lipophilicity, but also *pH* and ionization play an important role due to electrostatic forces between ions and negatively charged fatty acids in sebum (Yang et al., 2018). Here, we use a recently reported 2-D mechanistic *in silico* skin permeation mathematical model. The model has been validated recently in the literature for a variety of cases (Kattou et al., 2017; Sebastia-Saez et al., 2023). This methodology allows carrying out a complete parametric study for a set of virtual chemical compounds and isolate the effects of each parameter.

Table 1 Summary of published experimental studies on the effect of the FR on transdermal permeation of small molecules. ^aThe contribution of the FR on overall absorption was not reported in the experiment; rather, it was determined to be very small by an *in silico* study when the model provided good agreement with the plasma measurement [17]. ^bTwo values were obtained depending on the pH of the buffer solution used.

Reference	Test Condition	Compound(s)	MW [Da]	log $K_{o/w}$	Findings
Otberg et al. (2008)	<i>In vivo</i>	Caffeine	194	-0.07	The FR contributes to increased concentration in blood plasma ^a .
Teichmann et al. (2005)	<i>In vivo</i>	Sodium Fluorescein (SF)	376	-0.61	SF was recovered from follicular casts after experiment (3% of the dose was in the FR, 51% in corneocytes and the remainder was absorbed).
Teichmann et al. (2007)	<i>In vivo</i>	Curcumin	368	3.30	Curcumin permeates into the skin through lipid and FR.
Schwartz et al. (2011)	<i>In vivo</i>	Zinc pyrithione (ZP)	317	0.90	Significant amount of ZP detected in FR post-assay
Ossadnik et al. (2007)	<i>In vivo</i>	Brilliant green solution	484	2.02	Brilliant green solution detected in FR post-assay.
Grams and Bouwstra (2002)	<i>Ex vivo</i>	Bodipy FLc5	320	1.20	Bodipy FLc5 and Bodipy 564/570C5 detected in FR post-assay, but not Oregon Green 488
		Bodipy 564/570C5	463	3.00	
		Oregon Green 488	509	-2.50	
Chandrasekaran et al. (2016)	<i>In vitro</i>	Magnesium	23	-1.10	Magnesium permeates better into the skin when the FR is not blocked.
Genina et al. (2002)	<i>In vivo & in vitro</i>	Dye Indigo Carmine (IG)	466	3.72	Both substances were present in the FR after <i>in vivo</i> assays, but ICG permeates faster <i>in vitro</i> .
		Dye Indocyanine Green (ICG)	775	-0.29	
Frum et al. (2007)	<i>In vitro</i>	Estradiol	272	2.29	The FR does not show a clear relationship with the lipophilicity of the compound in this study.
		Corticosterone	346	1.94	
		Hydrocortisone	362	1.60	
		Aldosterone	360	1.08	
		Cimetidine	252	0.40	
		Deoxyadenosine	251	-0.55	
		Adenosine	267	-1.05	
Ogiso et al. (2002)	<i>In vitro</i>	Ketoprofen (KP)	254	3.12	Flux of KP much higher than that observed for MT and 5FU. Histological observations confirmed permeation had occurred through the FR.
		Melatonin (MT)	232	1.18	
		Fluorouracil (5FU)	130	-0.89	

Mohd et al. (2016)	<i>In vitro</i>	Fluorescein isothiocyanate-dextran	4000	-0.77	The follicular pathway clearly favoured the permeation of hydrophilic compounds, with a linear relationship between $\log K_{o/w}$ and contribution of the FR.
		Calcein sodium salt	644	-3.50	
		Fluorescein sodium salt	376	-0.61	
		Isosorbide dinitrate	236	1.23	
		Lidocaine hydrochloride	234	-0.9/1.4 ^b	
		Aminopyrine	231	-1/0.98 ^b	
		Ibuprofen	206	1.9/1.3 ^b	
		Butyl paraben	194	3.50	
		Isosorbide mononitrate	191	-0.15	
Essa et al. (2002)	<i>In vitro</i>	Estradiol	272	2.29	Greater contribution of the FR for hydrophilic than lipophilic compounds.
		Mannitol	182	-2.47	
		Liposomes	-		

2. Materials and Methods

The mechanistic mathematical model used in this work consists of a 2-D geometric representation of the skin layers, complemented with state-of-the-art QSPRs to calculate the diffusion and partition coefficients. The model is an adaptation of a previously published model (Kattou et al., 2017; Sebastia-Saez et al., 2023), to accommodate a configuration with an infinite dose in the vehicle and a sink in the receiver, used frequently in skin permeability lab work. Dimensions and boundary layers are represented in Figure 1. Cases with open, blocked, and closed FR were run to calculate the contribution of the FR to overall dermal permeability. In ‘blocked FR’ cases, flux through the concentration boundary of the FR was restricted to half that of the open FR cases to mimic the experimental conditions of Mohd et al. (2016). In ‘closed FR’ cases, the concentration boundary of the FR was replaced by a no flux boundary to suppress the flow from the vehicle directly into the FR.

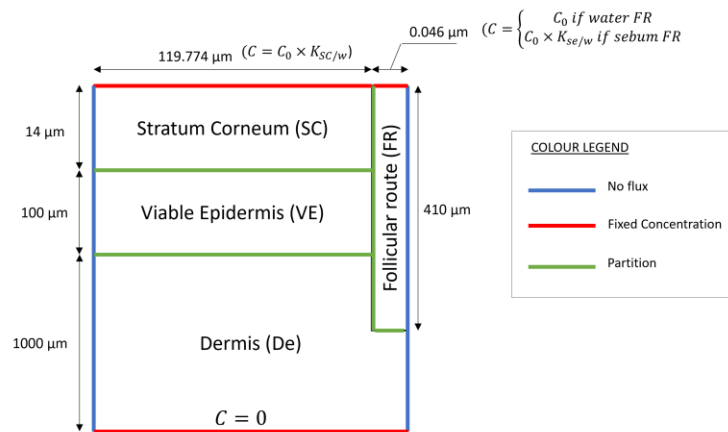


Figure 1 Schematic illustration of the computational domain including colour-coded boundary layers and dimensions. The figure includes only the case of open FR. Fixed concentration boundaries include their value for the cases with a FR filled with water or sebum. Not to scale.

A fixed concentration $C_0 = 1 \text{ mol/m}^3$ was fixed for the aqueous vehicle with infinite dose. The model solves the diffusion equation with no convection.

$$\frac{\partial c}{\partial t} + \nabla \cdot \vec{J} = 0 \quad (1)$$

where c denotes concentration, t denotes time, and \vec{J} is Fick's diffusive flux: $\vec{J} = -D\nabla c$, with D being the diffusion coefficient.

Diffusion and partition coefficients are needed for each layer to run the model. Recently reported QSPR models with improved coefficients of determination were used to obtain the partition coefficients and are summarised in Table 2.

Table 2 Summary of expressions used to calculate partition parameters. ^aVolume fractions and densities are $\varphi_{pro} = 0.1476$, $\varphi_{lip} = 0.0671$, $\varphi_w = 0.7853$, $\rho_{pro} = 1.37 \text{ g/cm}^3$, $\rho_{lip} = 0.90 \text{ g/cm}^3$, $\rho_w = 1.00 \text{ g/cm}^3$ and $\rho_{SC} = 1.05 \text{ g/cm}^3$ (Wang et al., 2010). ^bPartition coefficients calculated as $K_{pro/w} = 4.2 \times K_{o/w}^{0.31}$ and $K_{lip/w} = K_{o/w}^{0.69}$ (Wang et al., 2010).

Parameter	Expression
Partition coefficient SC to water ^{a,b} ($R^2 = 0.89$) (Wang et al., 2010)	$K_{SC/w} = \left(\varphi_{pro} \times \frac{\rho_{pro}}{\rho_w} \times K_{pro/w} + \varphi_{lip} \times \frac{\rho_{lip}}{\rho_w} \times K_{lip/w} + \varphi_w \right) \times \frac{\rho_w}{\rho_{SC}}$
Partition coefficient VE to water and De to water (Kretsos et al., 2018; Ibrahim et al., 2012)	$K_{VE/w} = 0.7 \times \left(0.68 + \frac{0.32}{f_u} + 0.025 \times f_{non} \times K_{o/w}^{0.7} \right)$
Partition sebum to water ($R^2 = 0.79$) (Yang et al., 2018)	$\log K_{se/w} = \log \left\{ f_{non} \times \left(\frac{1 + 0.71 \times 10^{pH-6.95}}{1 + 10^{pH-6.95}} \right) + f_{cat} \times \left(\frac{1.23 \times 10^{pH-6.95}}{1 + 10^{pH-6.95}} \right) \right\} + 0.79 \times \log K_{o/w}$

And the expressions used to calculate the diffusion coefficients are gathered in Table 3.

Table 3 Summary of expressions used to calculate diffusion parameters in SI units. ^aThe following expression (Mitragotri, 2002) was used to calculate the permeability of the SC ($K_p = 5.6 \times 10^{-6} K_{o/w}^{0.7} e^{-0.46r^2}$). Thickness of the SC is $\delta = 14 \mu\text{m}$ as indicated in Figure 1 (Kattou et al., 2017). Partition coefficient SC to water $K_{SC/w}$ calculated as indicated in Table 2. ^bPartition coefficient lipid to water was $K_{mw} = \frac{\rho_{lip}}{\rho_w} K_{o/w}^{0.69}$ (Chen et al., 2015). ^cMolecular radius $r = \sqrt[3]{3/4\pi \times 0.9087 \times MW}$ (Mitragotri et al., 1999). ^dBoltzmann constant $k_b = 1.380649 \times 10^{-23} \text{ J/K}$. Temperature $T = 20^\circ\text{C}$. Dynamic viscosity of water $\eta = 1.0016 \text{ mPa}\cdot\text{s}$.

Parameter	Expression
Diffusion coefficient in SC ^a	$D_{SC} = \frac{K_p \times \delta}{K_{SC/w}}$
Diffusion coefficient in VE and De ^b (Kattou et al., 2017)	$D_{VE} = \frac{10^{-8.15-0.655 \times \log MW}}{0.68 + \frac{0.32}{f_u} + 0.025 \times f_{non} \times K_{mw}}$
Diffusion coefficient in sebum ($R^2 = 0.92$) ^c (Yang et al., 2019)	$D_{se} = 2.48 \times 10^{-4} e^{-0.42 \times r^2}$
Diffusion coefficient in water (Stokes equation) (Einstein, 1905)	$D_w = \frac{k_b \times T}{6 \times \pi \times \eta \times r}$

The contribution of the follicular route (CFR) to skin permeability was calculated as:

$$CFR[\%] = \frac{P_{open} - P_{closed}}{P_{open}} \times 100 \quad (2)$$

where P represents permeability and is obtained by dividing the flux at steady state J over the concentration in the donor C_0 as $P = J/C_0$. The flux was obtained from the simulations when steady state was reached (variations below 0.1% across the domain). The calculation of one value of the parameter CFR requires two simulations: One with the FR open and another with the FR blocked as indicated in Figure 1.

The present model includes a homogeneous SC, as opposed to the versions of the model published by Kattou et al. (2017), which included the ‘bricks and mortar’ layout. The results in Kattou et al. (2017) for dermal absorption of caffeine with clearance were replicated here by including the homogenised SC to check the validity of the assumption.

From the expressions in Table 2 and Table 3, it can be derived that the calculation of *CFR* depends upon the parameters in Figure 2. The parametric study will be carried out by isolating the effect of these parameters. The simulations will be carried out for the cases of a hydrophilic (water) and lipophilic (sebum) FR, mimicking respectively, an *in vitro* and an *in vivo* scenario.

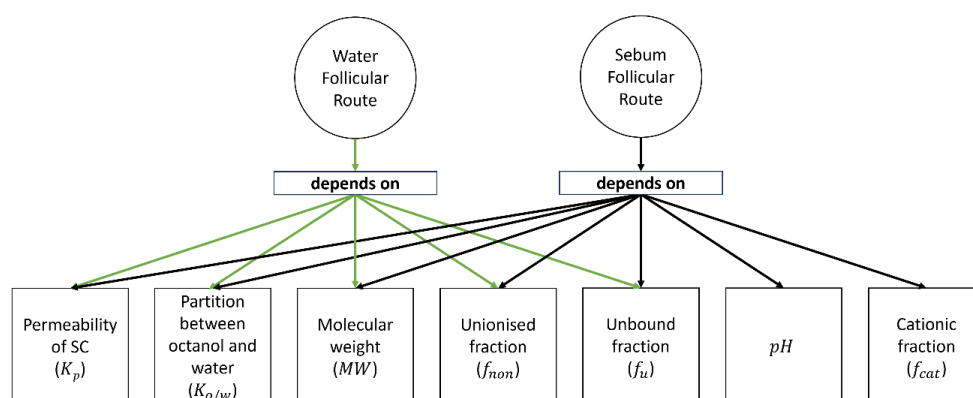


Figure 2 Summary of parameters varied in the parametric study for the cases of hydrophilic FR (filled with water, green arrows) and lipophilic FR (filled with sebum, black arrows).

For a water FR, simulations will be carried out for 11 values of $\log K_{o/w}$ in the range $[-3.70, 5.49]$. Two values of molecular weight (i.e., $MW = 50$ Da and 285 Da). These cover the range of values of a large number of commercial cosmetic and therapeutic drugs (Chen et al., 2013). The values of unbound f_u and non-ionized f_{non} fraction were 0 and 1. For each value of $\log K_{o/w}$, all possible combinations of molecular weight MW , unbound fraction f_u and non-ionised fraction f_{non} will be simulated. This makes a total of 88 virtual compounds (176 simulations for both blocked and unblocked FR).

A check was conducted on the uncertainty introduced by QSPRs used to compute the permeability of the SC due to low coefficient of determination ($R^2 = 0.58$). The contribution of the FR against $\log K_{o/w}$ was obtained for a set of chemicals with reported experimental measurements of the permeability (Chen et al., 2013) and compared with the QSPR prediction. The parameters of the chemicals implemented in these simulations are summarised in Table 4. An additional set of 120 simulations (water FR) was carried out to perform this check.

Table 4 Parameters of chemical compounds used in uncertainty check.

Compound	$\log K_{o/w}$	MW [Da]	Experimental $\log K_p$ [cm/s] [Chen et al., 2013]
Sucrose	-3.70	342	-8.84
Aspartic acid	-3.47	133	-7.43
Lysine	-3.05	146	-6.87
Histidine	-2.90	155	-7.82
Urea	-2.11	61	-7.39
Methanol	-0.77	32	-6.38
Ethanol	-0.31	46	-7.06
Nicotinic acid	0.36	123	-8.18
Barbital	0.65	184	-7.51
Aldosterone	1.08	360	-7.86

Codeine	1.19	299	-7.09
Pentanol	1.51	88	-5.78
Hexanol	2.03	102	-5.44
Salicylic acid	2.26	138	-5.07
Hydrocortisone methylsuccinate	2.60	477	-7.23
Naproxen	3.18	230	-4.97
Testosterone	3.32	288	-6.21
Progesterone	3.87	314	-5.43
Diclofenac	4.51	296	-5.30
Hydrocortisone octanoate	5.49	489	-4.76

The case of sebum FR depends on all the parameters varied for the water FR plus the cationic fraction f_{cat} of the compound and the pH . Two values of the cationic fraction (i.e., $f_{cat} = 0$ and 1) were tested. Two values of the pH were used (i.e., $pH = 4$ and 10), which cover all practical instances. In this case, the same values of $\log K_{o/w}$ are used as for the FR filled with water. Simulations for water FR were performed prior to sebum FR, and those parameters with no effect in the water FR were not considered for sebum FR. A set of 66 virtual chemical compounds was tested for sebum FR. This makes a total of 132 simulations considering the cases of non-ionised compounds, ionised cationic and ionised anionic for both values of the pH .

3. Results and Discussion

The simulations run to check the validity of the homogeneous SC assumption are gathered in Figure 3. The experimental results of Otberg et al. (2008) used by Kattou et al. (2017) for validation are included in the graph. The present simulations with homogenized SC used the experimental SC permeability of Johnson et al., 1997 ($D_{SC} = 4.12 \times 10^{-15} \text{ m}^2/\text{s}$), Abraham and Martins, 2004 ($D_{SC} = 4.73 \times 10^{-15} \text{ m}^2/\text{s}$) and the QSPR prediction by Mitragotri, 2002 ($D_{SC} = 4.73 \times 10^{-15} \text{ m}^2/\text{s}$). The data series compare well, hence providing validation of the homogeneous SC assumption.

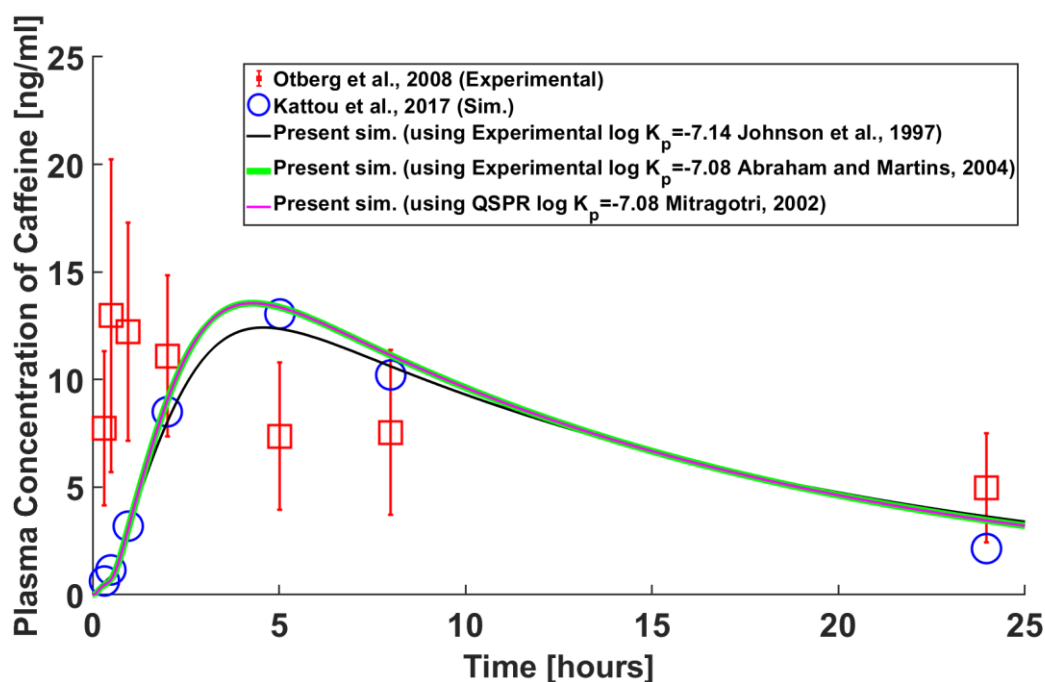


Figure 3 Comparison between results obtained using the 'bricks and mortar' SC layout (Kattou et al., 2017) for dermal absorption of caffeine with blood clearance and the replicated results using the homogenized SC assumption.

The results for a water FR are in Figure 4. An inverse relationship between the contribution of the FR and the octanol-to-water partition coefficient $\log K_{o/w}$ can be observed, confirming that a water FR favours the permeation of hydrophilic virtual compounds. Three areas can be distinguished on the graph. For hydrophilic compounds (i.e., $\log K_{o/w} < 1$), the contribution of the follicular path to the permeability of the skin is close to 50% regardless of molecular weight, percentage of protein binding and percentage of ionisation. Thus, most of the applied dose would permeate into the sink via the FR, hence by-passing the lipidic route in the SC. This is in accordance with the data of Mohd et al. (2016), who observed values of the *CFR* of around 50% for highly hydrophilic compounds in their experiments, suggesting a major contribution of the FR. For strongly lipophilic molecules (i.e., $\log K_{o/w} > 6$), the effect is the opposite; the proportion of the dose crossing into the sink via the FR is negligible due to its hydrophilicity. For molecules ranging from slightly hydrophilic to moderately lipophilic (i.e., $1 > \log K_{o/w} > 6$), a balance can be found between the epidermal and the FR.

The data shows that the molecular weight has an important impact, however, the trend observed remains unchanged for both values of *MW* tested. No effect of unbound f_u and non-ionized fraction f_{non} was observed. For a given value of the compound's lipophilicity, the contribution of the FR increases with the molecular weight regardless of protein binding and ionisation. Experimental observations in the literature suggest an inverse relationship between the permeability of the SC and molecular weight of the compounds (Mitragotri, 2002), which could result in the FR becoming more significant than the epidermal route to overall dermal permeation for increased *MW*. This is consistent with this simulated data, as the contribution of the FR is smaller for 50 Da than for 285 Da virtual compounds.

The simulated data is thus in accordance with the hypothesis by which physico-chemical changes might occur *in vitro*, that result in the FR favouring the permeation of hydrophilic compounds. The trend agrees with the experimental observations of Mohd et al. (2016), who observed an inverse relationship between the contribution of the FR to dermal permeability and $\log K_{o/w}$ for a set of compounds with varied molecular weights, binding properties and ionization characteristics. Frum et al (2007) recorded however an initial increasing trend in followed by a turning point and a sharp decrease. Their experimental observations show a significant *CFR* for highly hydrophilic compounds, and near-zero values for compounds with high $\log K_{o/w}$. In light of their results, it could be hypothesized that the FR was filled with water, or at least with a significant proportion of it, in their *in vitro* experiments.

Figure 5 shows the results of the uncertainty check introduced by Mitragotri's expression. The graph shows that the trend does not change regardless of whether experimental measurements (Chen et al., 2013) or Mitragotri's prediction of the SC permeability is used to calculate the diffusion coefficient in the SC. This simulated data was obtained for a set of real compounds with a range of values of molecular weight, protein binding properties and ionization characteristics for a water FR. The trend suggests thus that a water FR favours the permeation of hydrophilic compounds regardless of the other parameters, hence providing further evidence that the experimental *in vitro* results of Mohd et al. (2016) might have been obtained with a FR filled with a watery substance.

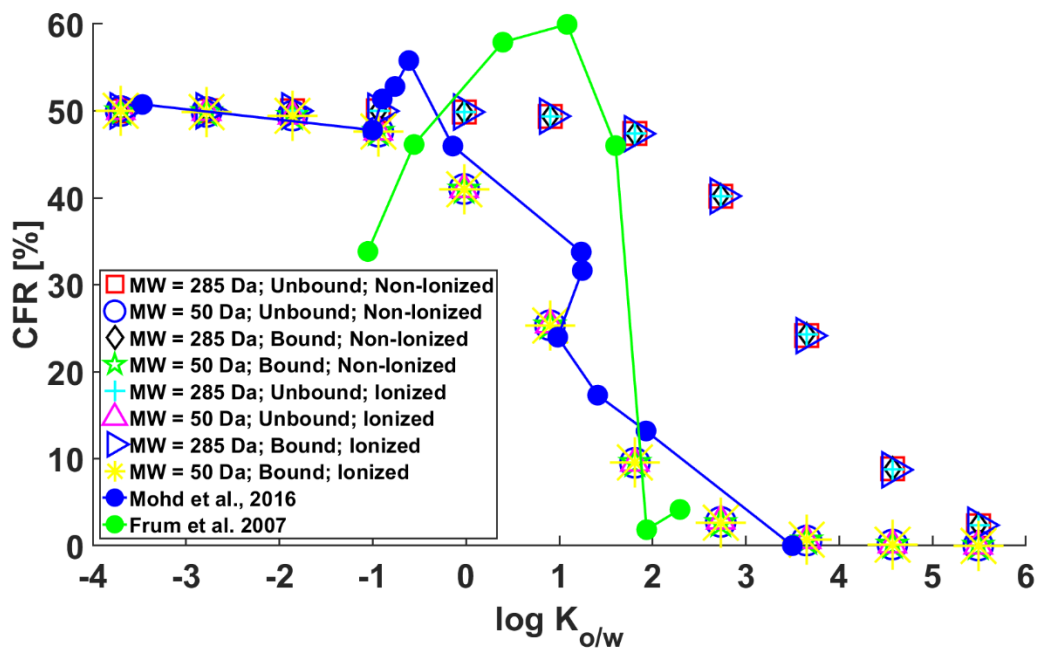


Figure 4 Percentage of contribution of the follicular route CFR against $\log K_{o/w}$ for water FR.

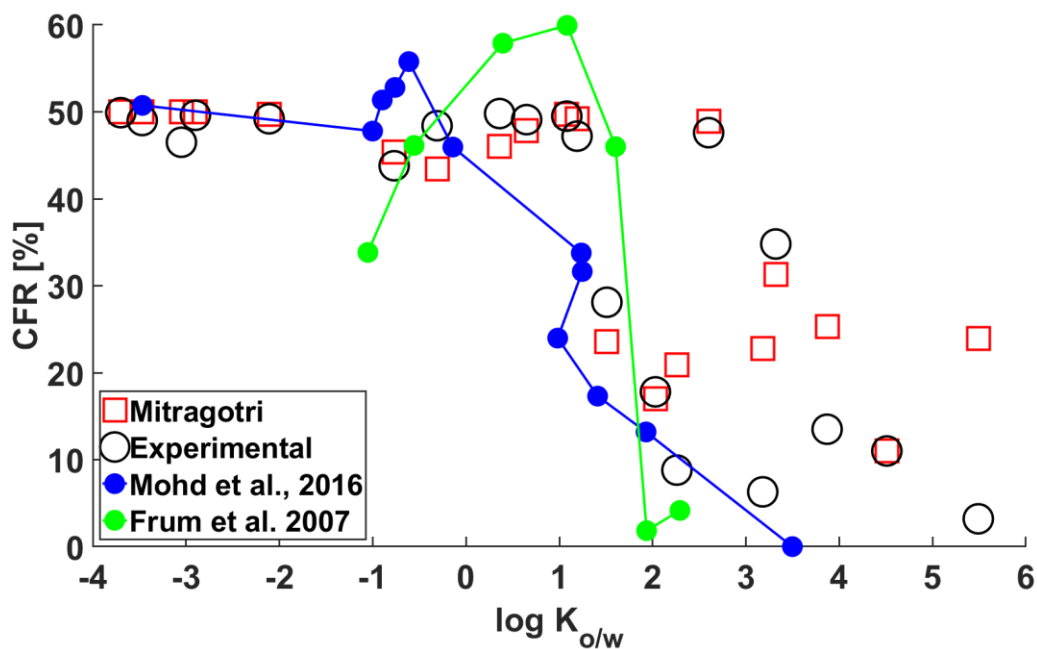


Figure 5 Percentage of contribution of the follicular route CFR against $\log K_{o/w}$ for Mitragotri's SC permeability uncertainty check.

The simulated skin permeability was compared with the experimental SC permeability for the set of chemical compounds in Table 4. The results of the comparison are included in Table 5. The simulated permeability of the skin with closed FR is the closest to the experimental data among the three simulated series, with slightly smaller permeabilities since the simulated cases add the contribution of the viable epidermis and dermis to the skin permeability. The skin permeability increases significantly for the results with blocked FR (i.e., flux restricted to half that of the open hair follicle) and open FR.

Table 5 Comparison between experimental measurement of the permeability of the SC and the simulated permeabilities of the skin for closed FR (no flux boundary between vehicle and FR), blocked FR (flux through concentration boundary of FR limited to half) and open FR.

Compound	Experimental $\log K_p$ [cm/s] [Chen et al., 2013]	Simulated Skin Permeability $\log K_{skin}$ [cm/s] for closed FR	Simulated Skin Permeability $\log K_{skin}$ [cm/s] for blocked FR	Simulated Skin Permeability $\log K_{skin}$ [cm/s] for open FR
Sucrose	-8.84	-8.89	-6.23	-5.93
Aspartic acid	-7.43	-7.47	-6.06	-5.77
Lysine	-6.87	-6.92	-6.04	-5.76
Histidine	-7.82	-7.86	-6.10	-5.80
Urea	-7.39	-7.42	-5.94	-5.64
Methanol	-6.38	-6.41	-5.75	-5.50
Ethanol	-7.06	-7.09	-5.88	-5.60
Nicotinic acid	-8.18	-8.22	-6.06	-5.76
Barbital	-7.51	-7.56	-6.12	-5.82
Aldosterone	-7.86	-7.92	-6.23	-5.94
Codeine	-7.09	-7.15	-6.17	-5.89
Pentanol	-5.78	-5.84	-5.63	-5.49
Hexanol	-5.44	-5.54	-5.43	-5.35
Salicylic acid	-5.07	-5.27	-5.22	-5.18
Hydrocortisone methylsuccinate	-7.23	-7.29	-6.25	-5.97
Naproxen	-4.97	-5.25	-5.22	-5.19
Testosterone	-6.21	-6.28	-5.95	-5.76
Progesterone	-5.43	-5.59	-5.51	-5.45
Diclofenac	-5.30	-5.48	-5.42	-5.37
Hydrocortisone octanoate	-4.76	-5.21	-5.19	-5.18

The results for a FR filled with sebum are in Figure 6. Variations in molecular weight and protein binding properties were not considered due to their negligible role in the water FR study. The data suggests an important role of ionization. The data trend shows that the FR grows in relevance as the lipophilicity of the virtual compound increases. At $\log K_{o/w} \approx 3.5$, there is a turning point in the trend. This is caused by smaller partition of strongly lipophilic compounds from the sebum FR and into the aqueous dermis than slightly lipophilic compounds. Retention in the sebum FR would thus impede flow into the sink, hence reducing the contribution of the FR to overall skin permeability. The data suggests a major role of the FR, with *CFR* greater than 40%, for non-ionized virtual compounds and highly dissociated ($pH = 10$) cationic compounds. Increased relevance of the FR is found for cationic than for anionic compounds and this can be explained by the presence of negatively charged fatty acids in the sebum FR.

Despite the observed turning point in the sebum FR data, the overall observation is that a sebum FR seems to favour the dermal permeability of lipophilic compounds, while a water FR favours the permeation of hydrophilic compounds. Variations in molecular weight, pH and compound ionization have a quantitative effect, although they do not modify the general trend.

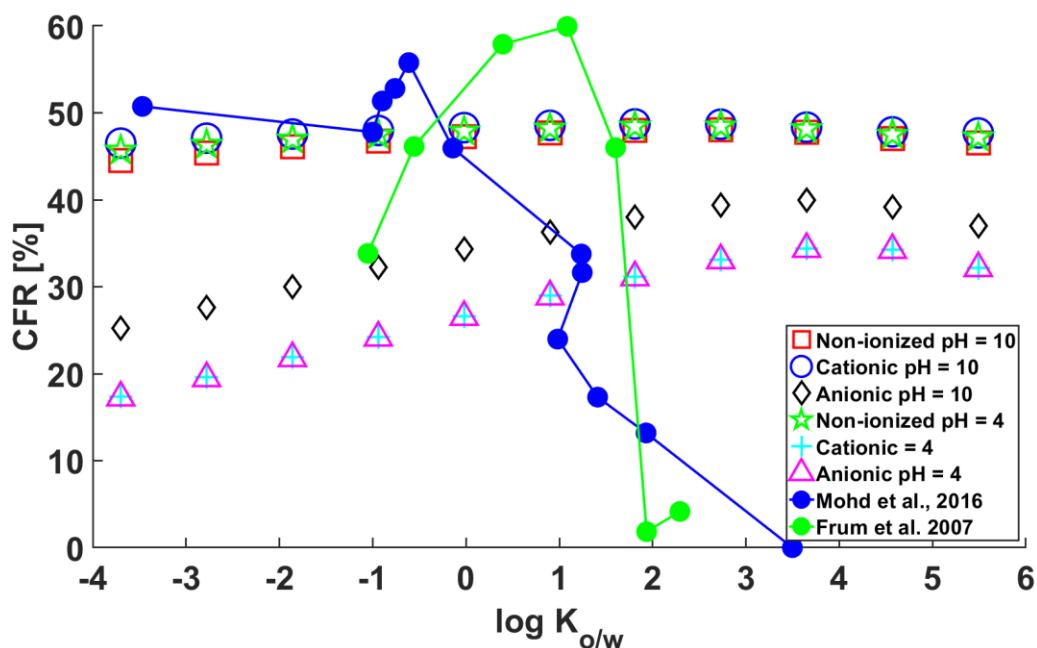


Figure 6 Percentage of contribution of the follicular route CFR against $\log K_{o/w}$ for sebum FR.

4. Conclusions

An *in silico* study has been carried out to quantify the effect of several parameters on the role that the follicular route has on overall dermal permeability, as information in the literature remains inconclusive regarding the role of the follicular route. The *in silico* methodology in this study allows the analysis of a wide range of potential dermal permeation scenarios by varying parameters that describe lipophilicity, protein binding, molecular weight and ionization.

The simulated data shows that the contribution of the follicular route can range from negligible to major if compared to the alternative epidermal route depending mainly on the appropriate combination of lipophilicity/hydrophilicity of both the substance filling the follicular route and the compound being administered. The molecular weight and other properties such as protein binding and ionization characteristics do not affect the general trend observed.

Variations in the composition of the substance filling the follicular route have thus a noticeable impact on the contribution of the follicular route to skin permeability. Uncontrolled modifications of the physico-chemical properties of the follicular route between *in vivo* and *in vitro* experimental conditions due to sample manipulation and cessation of vital functions may give rise to distorted interpretation of dermal permeation tests. Thus, determination of the composition of the substance that fills the follicular route would be advisable prior to dermal permeation experimental work.

REFERENCES

- Abraham MH, Martins F. Human skin permeation and partition: general linear free-energy relationship analyses. *J Pharm Sci.* 2004; 93:1508–1523.
- Chandrasekaran NC, Sanchez WY, Mohammed YH, Grice JE, Roberts MS, Barnard RT. Permeation of topically applied Magnesium ions through human skin is facilitated by hair follicles. *Magnes Res.* 2016; 29:35–42.

- Chen L, Han L, Lian G. Recent advances in predicting skin permeability of hydrophilic solutes. *Adv Drug Del Rev.* 2013; 65:295–305.
- Chen L, Han L, Saib O, Lian G. In silico prediction of percutaneous absorption and disposition kinetics of chemicals. *Pharm Res.* 2015; 32(5):1779–93.
- Einstein A. On the movement of small particles suspended in stationary liquids required by the molecular-kinetic theory of heat. *Ann Phys.* 1905; 322:549–60.
- Essa EA, Bonner MC, Barry BW. Human skin sandwich for assessing shunt route penetration during passive and iontophoretic drug and liposome delivery. *J Pharm Pharmacol.* 2002; 54:1481–90.
- Frum Y, Bonner MC, Eccleston GM, Meidan VM. The influence of drug partition coefficient on follicular penetration: in vitro human skin studies. *Eur J Pharm Sci.* 2007; 30:280–7.
- Genina E a, Bashkatov AN, Sinichkin YP, Kochubey VI, Lakodina N a, Altshuler GB, et al. In vitro and in vivo study of dye diffusion into the human skin and hair follicles. *J Biomed Opt.* 2002; 7:471–7.
- Grams YY, Bouwstra JA. Penetration and distribution of three lipophilic probes in vitro in human skin focusing on the hair follicle. *J Control Release.* 2002; 83:253–62.
- Ibrahim R, Nitsche JM, Kasting GB. Dermal clearance model for epidermal bioavailability calculations. *J Pharm Sci.* 2012; 101(6): 2094–108.
- Johnson ME, Blankschtein D, Langer R. Evaluation of solute permeation through the stratum corneum: lateral bilayer diffusion as the primary transport mechanism. *J Pharm Sci.* 1997; 86:1162–1172.
- Kattou P, Lian G, Glavin S, Sorrell I, Chen T. Development of a Two-Dimensional Model for Predicting Transdermal Permeation with the Follicular Pathway: Demonstration with a Caffeine Study. *Pharm Res. Pharmaceutical Research;* 2017; 34:2036–48.
- Knorr F, Lademann J, Patzelt A, Sterry W, Blume-Peytavi U, Vogt A. Follicular transport route – Research progress and future perspectives. *Eur J Pharm Biopharm.* 2009; 71:173–80.
- Kretsos K, Miller MA, Zamora-Estrada G, Kasting GB. Partitioning, diffusivity and clearance of skin permeants in mammalian dermis. *Int J Pharm.* 2008; 346(1–2):64–79.
- Mitragotri S. A theoretical analysis of permeation of small hydrophobic solutes across the stratum corneum based on scale particle theory. *J Pharm Sci.* 2002; 91(3):744–52.
- Mitragotri S, Johnson ME, Blankschtein D, Langer R. An analysis of the size selectivity of solute partitioning, diffusion, and permeation across lipid bilayers. *Biophys J.* 1999; 77:1268–83.
- Mohd F, Todo H, Yoshimoto M, Yusuf E, Sugibayashi K. Contribution of the Hair Follicular Pathway to Total Skin Permeation of Topically Applied and Exposed Chemicals. *Pharmaceutics.* 2016; 8:32.
- Ogiso T, Shiraki T, Okajima K, Tanino T, Iwaki M, Wada T. Transfollicular drug delivery: penetration of drugs through human scalp skin and comparison of penetration between scalp and abdominal skins in vitro. *J Drug Target.* 2002; 10:369–78.
- Ossadnik M, Czaika V, Teichmann A, Sterry W, Tietz H-J, Lademann J, et al. Differential stripping: introduction of a method to show the penetration of topically applied antifungal substances into the hair follicles. *Mycoses.* 2007; 50:457–62.
- Otberg N, Patzelt A, Rasulev U, Hagemeister T, Linscheid M, Sinkgraven R, et al. The role of hair follicles in the percutaneous absorption of caffeine. *Br J Clin Pharmacol.* 2008; 65:488–92.

Schwartz JR, Shah R, Krigbaum H, Sacha J, Vogt A, Blume-Peytavi U. New insights on dandruff/seborrheic dermatitis: The role of the scalp follicular infundibulum in effective treatment strategies. *Br J Dermatol*. 2011; 165:18–23.

Sebastia-Saez D, Benaouda F, Lim CH, Lian G, Jones SA, Cui L, Chen T. In-silico modelling of transdermal delivery of macromolecule drugs assisted by a skin stretching hypobaric device. *Pharmaceutical Research* 2023; 40(1):295–305.

Teichmann A, Jacobi U, Ossadnik M, Richter H, Koch S, Sterry W, et al. Differential Stripping: Determination of the Amount of Topically Applied Substances Penetrated into the Hair Follicles. *J Invest Dermatol*. 2005; 125:264–9.

Wang L, Chen L, Lian G, Han L. Determination of partition and binding properties of solutes to stratum corneum. *Int J Pharm* [Internet]. Elsevier B.V.; 2010; 398:114–22. Available from: <http://dx.doi.org/10.1016/j.ijpharm.2010.07.035>.

Yang S, Li L, Chen T, Han L, Lian G. Determining the Effect of pH on the Partitioning of Neutral, Cationic and Anionic Chemicals to Artificial Sebum: New Physicochemical Insight and QSPR Model. *Pharm Res. Pharmaceutical Research*; 2018; 35.

Yang S, Li L, Lu M, Chen T, Han L, Lian G. Determination of Solute Diffusion Properties in Artificial Sebum. *J Pharm Sci* [Internet]. Elsevier Ltd; 2019; 108:3003–10. Available from: <https://doi.org/10.1016/j.xphs.2019.04.027>.